

## The experimental relation between the tearing mode growth rate and the perturbed magnetic field

F. Salzedas, A.A.M. Oomens, F.C. Schüller and the RTP team

*FOM-Instituut voor Plasmafysica 'Rijnhuizen', Association Euratom-FOM, Trilateral Euregio Cluster, P.O. Box 1207, 3430 BE Nieuwegein, The Netherlands*

### Introduction

In this paper we will analyze experimental observations of the evolution of an  $m/n = 2/1$  tearing mode that grows prior to density limit disruptions in RTP ( $R/a = 0.72/0.164$  m,  $B_\phi < 2.5$  T,  $I_p < 150$  kA). To provoke the disruptions the density was ramped in ohmic He discharges, using a Ne gas puff. With Ne puff the radiative density limit could be kept below the cut-off density of the heterodyne radiometer and moreover the discharges were more reproducible. Besides, density limit disruptions provoked with Ne showed the same features as density limit disruptions provoked with other gases. Plasma currents were typically  $I_p = 100$  kA with  $q_a \approx 4$ . In discharges where sawteeth are observed through out the plasma current flat top (the most frequent ones) the electron density increases monotonously and the edge temperature has an inverse behavior, as a result of the energy lost by radiation. In these discharges density limit disruptions are always preceded by an  $m/n = 2/1$  tearing mode that prior to the disruption shows an exponential increase in the amplitude for a period of less than 1 ms.

### Evolution of the $m = 2$ mode amplitude

During these precursors, when Ne is used as the puffing gas, it is observed that before the amplitude of the  $m = 2$  mode starts to increase exponentially the mode grows algebraically for a time of the order of the global resistive time,  $\tau_R$ , that can vary between  $\approx 10 - 20$  ms. The mode amplitude is very small during this phase and its time evolution is best observed through the perturbations in the poloidal magnetic field,  $\tilde{B}_\theta$ , measured by pick-up coils. During this phase the amplitude of  $\tilde{B}_\theta$  does not increase monotonously. Instead it shows a irregular modulation that has some correlation with the sawteeth and changes during small periods of  $\approx 1 - 2$  ms where the maximum value reached during each of these periods increases algebraically with time. We will refrain from giving a detailed description of this complex behavior. Instead, in this paper we will concentrate on the last millisecond before the disruption. It is in this period that the mode amplitude grows exponentially and becomes large enough to leave a clear mark of an  $m/n = 2/1$  mode, on the electron temperature profile.

One of the difficulties on the analysis of the behavior of these modes is to relate the measured  $\tilde{B}_\theta(r_c)$ , where  $r_c$  is the radius of the coils, with the unknown  $\tilde{B}_\theta(r_s)$  at the mode resonant surface, that is the quantity whose dynamics is predicted by theory. The usual procedure consists on approximating the toroidal plasma to a cylindrical one and then use the current profile as found from equilibrium codes, and solve the MHD equations using  $\tilde{B}_\theta(r_c)$  as a boundary condition, to find  $\tilde{B}_\theta(r_s)$ . An even more simple approach, that can be used as a simple estimation of  $\tilde{B}_\theta(r_s)$ , consists on neglecting the plasma current outside the resonant surface. In this case the  $m$  component of  $\tilde{B}_\theta(r_c)$  is related to  $\tilde{B}_\theta(r_s)$  by,

$$\tilde{B}_{\theta m}(r_c) = \tilde{B}_{\theta m}(r_s) \left( \frac{r_s}{r_c} \right)^{(m+1)} \frac{1 + \left( \frac{r_c}{r_w} \right)^{2m}}{1 - \left( \frac{r_s}{r_w} \right)^{2m}}, \quad (1)$$

where  $r_w$  is the radius of the wall of the vessel.

Here we will use an other method to measure the amplitude of the perturbations, directly and locally around the resonant surface. Basically, it relies on the assumption that close and

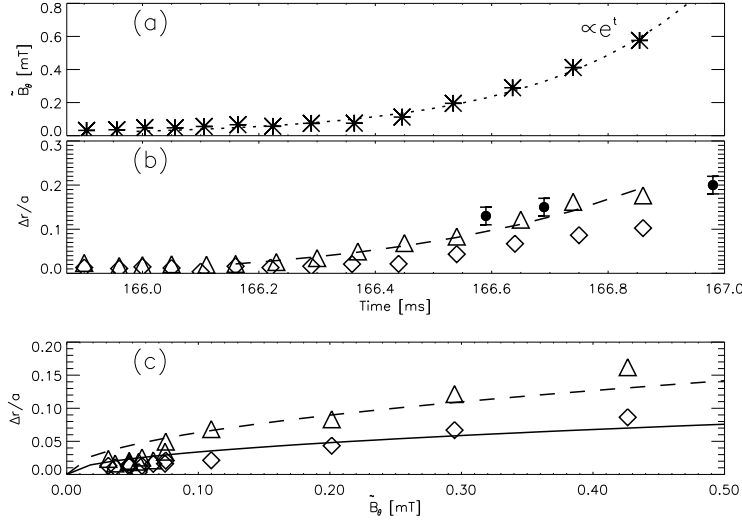


Figure 1: (a)  $\tilde{B}_\theta$ , (b)  $\Delta r/a$ . The three black circles indicate the island width estimated from the TS (see Fig. 2(a)). (c)  $\Delta r/a$  plotted against  $\tilde{B}_\theta$ . The symbols  $\Delta$  ( $\diamond$ ), refer to the low field side (high field side).

outside of the separatrix of a tearing mode the electron temperature is a flux function. In this case a change  $\Delta w$  of the island width will cause a proportional displacement  $\Delta r$ , of the flux surfaces in the neighborhood of the separatrix. The displacement  $\Delta r$  is given by,

$$\Delta r = \frac{\Delta T}{\frac{dT_0}{dr}}, \quad (2)$$

where  $T_0$  is the unperturbed temperature profile, measured along the X point and  $\Delta T$  is the difference in temperature between the point that is at the same angle of the X point and the point that is at the same angle of the O point. It is also implicitly assumed that the plasma is incompressible, which is the case, as long as the growth rate of the perturbation is smaller than the sound velocity in the plasma.

Figure 1(b) shows  $\Delta r/a$  derived both from the low field side (LFS, channel 6 see Fig. 2(c)) and on the high field side (HFS, channel 16). Between 166.2 ms and 166.8 ms,  $\Delta r$  increases exponentially. The statistical error in  $\Delta r$  is unknown because only one measurement per time step is available. More confidence on the measurement of  $\Delta r$  can be obtained from the observation of the full  $T_e$  profile, as shown on Fig. 2(c), where a characteristic of  $m = 2$  islands in tokamaks is visible, namely that the deformation of isothermals is symmetric in relation to the resonant surface on the HFS. On the LFS it is always difficult to localize the X point, since the island seems to grow towards the center of the plasma. In this case it would be expected that on the LFS  $\Delta r \simeq w$  while on the HFS  $\Delta r \simeq w/2$ . As shown on Fig. 1(b) this relation is verified with  $\Delta r(\text{LFS}) \simeq 2\Delta r(\text{HFS})$ . Moreover the estimated island width from the Thomson Scattering (TS) comes very close to the values of  $\Delta r$  measured on the LFS (see Fig. 1(b), and Fig. 2(a))<sup>1</sup>. The shape of both  $T_e$  and  $n_e$  TS profiles inside the mode is neither flat neither monotonous but irregular. Moreover in the third TS profile that is practically at the onset of the disruption,  $n_e(r)$  is shifted relatively to  $T_e(r)$  inside the mode. In Fig. 1(c)  $\Delta r$  is plotted against  $\tilde{B}_\theta$ , for values up to 19% of the minor radius, that are measured up to 100  $\mu\text{s}$  before the onset of the disruption. The best fits to the data give for the LFS and HFS,

$$\Delta r(\text{LFS}) = 1.04\sqrt{\tilde{B}_\theta}, \quad (3)$$

$$\Delta r(\text{HFS}) = 0.56\sqrt{\tilde{B}_\theta}. \quad (4)$$

<sup>1</sup>Although TS profiles have very high spatial resolution, the lack of time evolution hinders the precise location of the separatrix. The same difficulty occurs for the ECE radiometer where despite the high temporal resolution the low spatial resolution blurs the location of the separatrix.

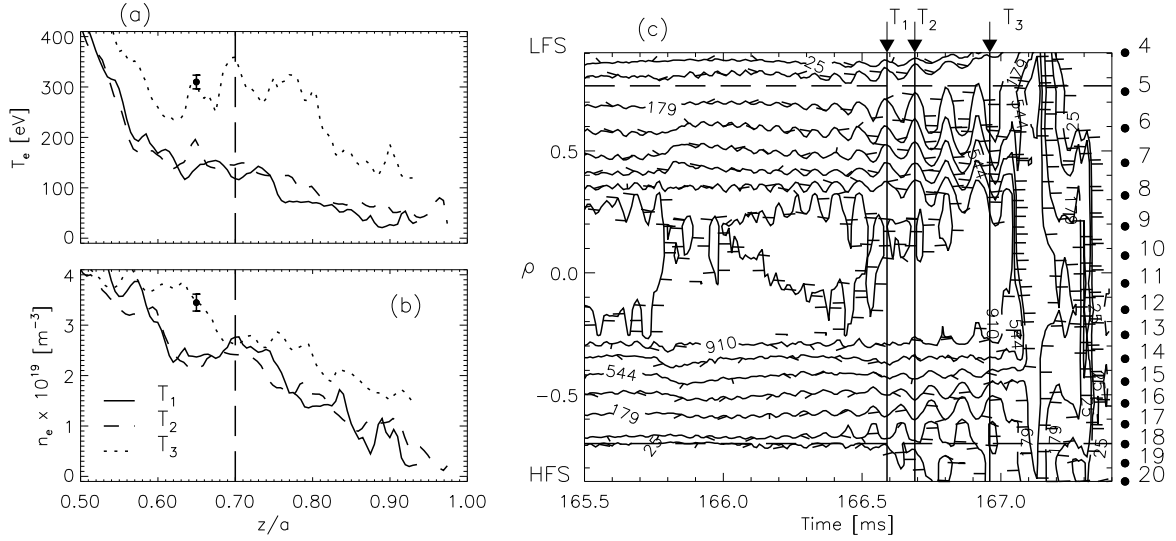


Figure 2: (a)  $T_e$  and (b)  $n_e$  high resolution TS temperature profiles measured at the indicated times in (c). Only the profile around  $q = 2$  is shown. For clarity just one typical error bar is shown. The vertical dashed line indicates the calculated radial position of the  $q = 2$  surface. (c) Time evolution of the radial temperature profile measured from the ECE radiometer. The channel numbers and its positions are indicated at the right.

The factor of 1.86 between the two fitting parameters just reflects once more the above mentioned relation  $\Delta r(\text{LFS}) \simeq 2\Delta r(\text{HFS}) \simeq w$ .

Therefore we should compare the experimental relation eq. 3 with the well known expression for the island width,

$$w = 4\sqrt{\frac{r_s q}{m B_\theta q'}} \sqrt{\tilde{B}_r} = 4\sqrt{\frac{r_s}{B_\theta q'}} \left(\frac{r_c}{r_s}\right)^{3/2} \sqrt{\frac{1 - \left(\frac{r_s}{r_w}\right)^4}{1 + \left(\frac{r_c}{r_w}\right)^4}} \sqrt{\tilde{B}_\theta(r_c)} \quad (5)$$

where eq. 1 was used with  $m = 2$ .

Using the values from table 1 that were calculated from the Thomson profile of Fig. 2(b) assuming that the current density  $j \propto T_e^{3/2}$  it is obtained,

$$w = 1.14 \sqrt{\tilde{B}_\theta(r_c)}. \quad (6)$$

The agreement between eq. 6 and the experimentally derived eq. 3 is very good. This indicates that toroidal effects that were neglected to obtain eq. 6 are not significant.

The signal of  $\tilde{B}_\theta$  was measured by just one coil that can measure signals with a frequency up to 500 kHz without attenuation. This means that  $\tilde{B}_\theta$  has more than just the  $m = 2$  component, however from the analysis of an array of slower pick-up coils it was found that the  $m = 2$  component is dominant.

One other important feature that can be seen in Fig. 1(c), is that during the period in which the mode grows exponentially up to 100  $\mu$ s before the disruption, the island width is proportional to  $\sqrt{\tilde{B}_\theta}$ . Therefore no significant changes occur in the equilibrium parameters,  $B_\theta(r_s)$ ,  $r_s$  and  $q'(r_s)$ . This is a clear and straightforward demonstration that eq. 5 is still valid up to island sizes of the order of 20% of the minor radius. This feature should be stressed because until now the support for eq. 5 on island sizes of this magnitude was only based on the magnetic measurements performed outside the plasma, that were afterwards extrapolated inwards up to the resonant surface indirectly via the MHD equations and transport codes.

| $T_e$<br>eV | $n_e$<br>$10^{19} \text{ m}^{-3}$ | $p_e$<br>kPa | $j$<br>$\text{MA m}^{-2}$ | $q'$<br>$\text{m}^{-1}$ | $B_\theta$<br>T | $\eta$<br>$10^{-6} \Omega \text{ m}$ | $\chi_\perp^{global}$<br>$\text{m}^2 \text{ s}^{-1}$ |
|-------------|-----------------------------------|--------------|---------------------------|-------------------------|-----------------|--------------------------------------|--|
| 127         | 2.67                              | 0.541        | 0.211                     | 32.7                    | 0.165           | 4.12                                 | 1.9  |

 Table 1: *Equilibrium parameters at  $r_s = 0.113$  m calculated from the  $T_1$  profile in Fig. 2.*

### Interpretation of the $m = 2$ mode evolution

In what follows we will apply the extended Rutherford model[1], that takes into account perturbations of the resistivity inside the mode, to the observations previously described. From this model the following relation was derived for the mode growth rate,

$$\frac{dw}{dt} = C_1 \frac{\eta}{\mu_0} \Delta' - C_2 \frac{\tilde{P}_T}{\chi_\perp T_e} w, \quad (7)$$

where  $C_1 = 1.22$  and  $C_2 = 0.9\eta j_z q / (B_\theta q')$  with all the quantities taken at the resonant surface.  $\tilde{P}_T$  is the total power density per particle in the island,  $\chi_\perp$  is the effective perpendicular electron thermal conductivity within the magnetic island and  $T_e$  is the temperature at the X point. The exponential growth can be explained by the sudden onset of the second term of eq. 7 with  $\tilde{P}_T < 0$ . An abrupt negative value of  $\tilde{P}_T$  is perfectly possible due to the nature of radiative power losses. Once the average temperature on the O point is low enough such that radiative recombination of this impurities can occur, energy inside the island will be lost by radiation at a much faster rate than by the usual transport mechanisms of energy in a plasma.

From the data of Fig. 1(b) it is possible to estimate the ratio of  $\tilde{P}_T / \chi_\perp$ . For that it will be assumed that  $\tilde{P}_T$  is constant during the short time interval in which the mode grows exponentially. Then, integration of eq. 7 gives,

$$w(t) = \frac{a_1}{a_2} + \left( w_0 - \frac{a_1}{a_2} \right) e^{-a_2 t}, \quad (8)$$

where  $a_1 = C_1 \frac{\eta \Delta'}{\mu_0} = 8 \text{ ms}^{-1}$ ,  $w_0 = w(t = 166.2 \text{ ms}) = 0.02 a$  and  $a_2 = \frac{C_2 \tilde{P}_T}{T_e \chi_\perp}$ . Fitting eq. 8 to the data of Fig. 1(b) (dashed line) it was found  $a_1 = 8 \text{ ms}^{-1}$  and  $a_2 = 2.3 \times 10^3 \text{ s}^{-1}$ . Then using  $a_2$  and the data of Table 1 it is found,  $\tilde{P}_T / \chi_\perp = 1.0 \times 10^6 \text{ eV m}^{-2}$ .

During the 0.6 ms of the exponential growth the temperature inside the island drops 150 eV which implies that  $\tilde{P}_T \approx 2.5 \times 10^5 \text{ eVs}^{-1} \text{ per particle}$ . So  $\chi_\perp^{island} = 0.25 \text{ m}^2 \text{ s}^{-1}$ . Comparing with  $\chi_\perp^{global}$  from table 1 it comes that  $\chi_\perp^{island} = 1/8 \chi_\perp^{global}$ .

In conclusion it was measured in RTP, that  $w \propto \sqrt{\tilde{B}_\theta}$  for  $0 \lesssim w \lesssim 20\% a$  and that the cylindrical approximation gives very good results if  $j_z(r > r_s)$  can be neglected. The Rutherford extended model accounts very well for the exponential growth and it implies that the effective  $\chi_\perp^{island}$  is 8 times smaller than  $\chi_\perp^{global}$ . It was also observed that inside the island the  $T_e$  profile is irregular and increases just before the disruption. At the same time the  $n_e$  profile shifts relatively to the  $T_e$  profile.

### Acknowledgments

The author F.Salzedas is supported by the Programa PRAXIS XXI. This work was performed under the EURATOM-FOM association agreement, with financial support from NWO and EURATOM.

### References

- [1] RUTHERFORD, P.H., *PPPL Report-2277*, (1985).